Diffusion of Large Flexible Polymer Chains through Model Porous Membranes

G. Guillot, L. Léger,* and F. Rondelez

Physique de la Matière Condensée,† Collège de France, 75231 Paris Cédex 05, France.
Received March 1, 1985

ABSTRACT: The diffusion of large polymer molecules through model porous membranes (pore radius R_P) has been measured as a function of both polymer concentration and molecular weight. In the limit of low concentrations, the parameter that controls the diffusion of the chains is their hydrodynamic radius R_H: for $R_H > R_P$, the diffusion is highly hindered. When the concentration is increased, our results demonstrate the existence of a new transport regime in which chains with $R_H > R_P$ can diffuse through the membrane with an effective diffusion coefficient, D_{eff}, 2 orders of magnitude larger than in the dilute concentration range. We interpret this behavior in the framework of the scaling approach to polymer solutions and show that this enhanced diffusion may be attributed to the concentration dependence of the partition coefficient between bulk solution and pores and is related to the flexibility of the chains.

Introduction

Transport of macromolecular solutes through porous media controls a wide variety of experimental situations such as gel permeation chromatography, ultrafiltration, and enhanced oil recovery.

A basic initial and intuitive idea was that solutes of size comparable to the pore radius could hardly penetrate the porous media. This simple geometrical view is well supported by a large amount of experimental data on diffusion or flow of rigid proteins and small molecular weight polymer solutions through a wide variety of porous media (compacted silica beads,[1] leached vycor glass,[2,3] mica or polycarbonate track-etched membranes with cylindrical pores[4-8]). Large flexible macromolecules, however, seem to deviate from this straightforward hard-sphere behavior and have been shown to penetrate small pores more easily than rigid particles.[2,5] Moreover, an enhancement of the permeation rate of flexible molecules has been observed in a few cases when either the flow rate or the polymer concentration are increased.[9-12]

From a theoretical point of view, Casassa was the first to calculate the partition coefficient (i.e., the ratio of the solute concentration inside the pore to the solute concentration outside) for both ideal flexible chains and rigid rods at infinite dilution from a statistical analysis of the polymer conformation.[13] Taking advantage of the scaling approach to polymer solutions, Daoud and de Gennes have investigated the conformations of large flexible chains in good solvent trapped into small cylindrical pores as a function of polymer concentration.[14] Daoudi and Brochard[15] have later evaluated the partition coefficient both in the very dilute regime and in the high- concentration regime where the chains become entangled inside the pore. Also, de Gennes and Brochard have calculated the diffusion coefficient of isolated chains inside a cylindrical pore[16] and Daoudi and Brochard have studied the transport under flow.[15]

Both approaches, static and dynamic, predict that large flexible chains penetrate small pores much more easily when the concentration is increased. Available experimental data seem in qualitative agreement with such prediction,[10,11,12,17] but quantitative comparisons are difficult to handle, as they suppose both well-defined polymer chains (low polydispersity, good solvent conditions) and well-defined porous geometry (cylindrical pores of controlled radius). Nuclepore filters (track-etched membranes) provide such controlled systems, but their porosity, fixed by the manufacturer's specifications, is generally too large for our needs.

We have thus undertaken a series of experiments using high molecular weight, low polydispersity polymers, and membranes similar to Nuclepore filters but prepared by ourselves in order to adjust their characteristics as desired, avoid pore overlap, and control the pore diameter. We have paid special attention to the case where the chain size, as defined by the hydrodynamic radius R_H, is comparable to the pore size R_P.

In the present paper, we examine the influence of both molecular weight and concentration of the solutions on the diffusion of the chains through the membranes in the absence of solvent flow. Our results on transport under flow will be presented in a forthcoming paper.

Experimental Procedures

1. Membranes. The detailed preparation and characterization of the membranes have been described previously,[18] and we summarize here only the main features. Polycarbonate films are irradiated with heavy Kr^{25+} ions, accelerated to an energy of 500 MeV or 6 MeV/N at A.L.I.C.E. synchrotron in Orsay. Under such high incident energies, latent tracks are formed in the film and later chemically etched to produce cylindrical pores spanning the membrane. The pore density is fixed by the irradiation dose, while the pore radius is governed by the duration of etching. Three techniques have been used to characterize the membranes; they are discussed below.

(a) Conductivity Measurements. The polycarbonate film has a high electrical resistivity, while the etching solution is an electrolyte (sodium hydroxide 2 N). The conductance σ of the membrane is related to the overall pore area and can be followed directly in the etching cell. If the pore density is known, an average value of the pore radius $R_P \sim \sigma^{1/2}$ can be extracted. A typical evolution of R_P vs. the etching duration is shown in Figure 1. Three time domains can be distinguished: (i) for $t < t_0$ the conductance is that of an unirradiated film and $R_P = 0$; (ii) at t_0 the first pores start to be broken through and R_P increases rapidly; (iii) at longer times ($t > t_1$) R_P increases linearly with etching time.

We can define the etching rate along the track as $v_T = L/t_0$, where L is the membrane thickness, and the bulk etching rate (for $t > t_1$) as $v_B = dR_P/dt$. The ratio v_T/v_B controls the final shape of the pores (cylindrical or conical) and can be made as large as 10^4 if the membranes are exposed to ultraviolet light before the etching.[19,20] With $v_T/v_B = 10^4$, one obtains cylindrical pores with $R_P = 10$ nm and $L = 10$ μm.

As discussed in ref 18, the determination of the overall pore area by conductivity has a good sensitivity for porosities smaller than 0.1% only. The calibration of the pore growth kinetics $R_p(t)$ has thus been performed with membranes of such a low porosity and by using an independent determination of v_B by weight-loss measurements of unirradiated samples.

† Unité associée au CNRS No. 792.

0024-9297/85/2218-2531$01.50/0

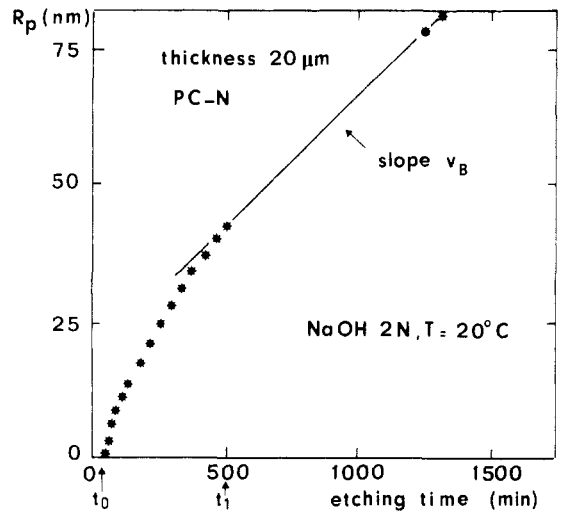

Figure 1. Evolution of the average pore radius R_P with etching time, t, as measured by the conductance ($R_P \propto \sigma^{1/2}$). At $t = t_0$ the first pores are broken through. For $t > t_0$, R_P increases with time, first in a rapid nonlinear way and then linearly. The bulk etching rate ($t > t_1$) is given by the slope of the linear region, $v_B = 2.4 \times 10^{-2}$ nm/min.

(b) Scanning Electron Microscopy (SEM). Direct observations of the etched membranes with a scanning electron microscope (after deposition of a thin gold or palladium–gold film, thickness 10 nm) provide three kinds of information: (i) pore density, a parameter determined by the irradiation dose and that is not under precise control during the irradiation; typically the uncertainty on the pore density is 20%, mainly due to the difficulty of analyzing a large enough number of pictures to get good statistics; (ii) pore size and pore size distribution; and (iii) etching rate v_B, from an analysis of the pictures taken at different etching times. The v_B values are in complete agreement with those deduced from the conductivity and the weight-loss measurements. The R_P values deduced from SEM are systematically smaller, by about 20 nm, than those deduced from conductivity. We have as yet no consistent explanation for this discrepancy. For $R_P <$ 50 nm the observed pore size becomes very inhomogeneous, probably because of the partial crystallinity of our polycarbonate samples (Markrofol KG and N from Bayer).

(c) Pure Solvent Permeability. The flow rate of different solvents (alcohol, ethyl acetate, cyclohexane) through the membranes has been measured under constant pressure head (0.1–1 bar) in Poiseuille flow conditions. The pore radii thus found are in close agreement (within 2%) with those derived from electrical measurements for $R_P > 50$ nm when the two measurements are made on the same membrane, in order to avoid the uncertainty due to fluctuations in the pore density. Since these two methods yield $\langle R_P^4 \rangle$ and $\langle R_P^2 \rangle$, respectively, this implies a narrow pore size distribution.

In all the following, the given R_P values are deduced from conductivity or permeability data, with a relative uncertainty of 2%.

2. Polymer Solutions. Narrow polystyrene fractions from Toyo Soda were dissolved in freshly distilled ethyl acetate, a solvent that does not alter the membrane properties.[10] The concentrations were determined by weighing, and the solutions were allowed to homogenize for more than 2 weeks under gentle intermittent agitation.

The hydrodynamic radius of the chains R_H was measured by quasi-elastic light scattering (QELS) using low concentration solutions (typically 10^{-4} g/g) after filtration through membranes of pore radius 100 nm or centrifugation (10^3 g for 0.5 h). For each molecular weight, we checked that the relaxation time τ of the correlation function of the scattered light was inversely proportional to the square of the scattering vector, q. For homodyne detection, $\tau = 3\pi\eta R_H/(k_B T q^2)$, where η is the solvent viscosity. Special care was taken to stay in the range $qR_H < 1$. The R_H values obtained are listed in Table I. Two important results must be pointed out: (i) Our R_H values are compatible with a scaling law $R_H \sim M_z^{0.55+0.02}$, showing that for these high molecular weights ethyl acetate is a good solvent for polystyrene. The same exponent was obtained by Adam and Delsanti for polystyrene in benzene.[21] (ii) Comparison of R_H values measured after sedimentation or filtration through the membranes shows that the filtration does not drastically affect the average molecular weight of the chains.

Finally, we have checked that no significant adsorption of polystyrene chains was taking place on the pore surfaces by measuring the permeability of the membranes to pure solvent before and after a 1-week incubation in the polymer solutions. The absence of adsorption was also confirmed by incubating the membranes in solutions of polystyrene covalently labeled with fluorescent anthracene groups and by monitoring the fluorescence intensity after intensive rinsing. This method would have detected adsorbed chains at surface densities as low as 2×10^{-2} μg/cm^2.

Table I
Characteristics of the Polystyrene Samples Used[a]

M_W	M_W/M_N	R_H, nm (T = 20 °C)	c^*, g/g
1.07×10^5	1.01	7.9 ± 0.4[b]	1.3×10^{-1}
7.75×10^5	1.01	22 ± 1[b]	2.6×10^{-2}
2.89×10^6	1.09	40 ± 4[c]	9×10^{-3}
6.77×10^6	1.14	58 ± 3[d]	4.6×10^{-3}
		58 ± 2[e]	
8.42×10^6	1.17	74.5 ± 2[d]	3.8×10^{-3}
		69 ± 5[b]	
		66 ± 2[e]	
20.6×10^6	unknown	110[f]	1.9×10^{-3}

[a] The polydispersity indexes M_W/M_N are from Toyo Soda specifications. The hydrodynamic radii R_H have been deduced from QELS by using the viscosity of ethyl acetate at 20 °C, $\eta = 0.455 \times 10^{-2}$ P. Indicative values of the first overlap concentration c^* have been calculated from $c^* = M_W/\rho N_A R_G^3$ and static light scattering measurements of the radius of gyration[26] by using the scaling law $R_G \propto M_W^{3/5}$. ρ is the solvent density and N_A Avogadro's number. [b] Dust removed by filtration (R_p = 100 nm). [c] Dust removed by filtration (R_p = 50 nm). [d] Dust removed by centrifugation. [e] Measured after passive diffusion (R_p = 75 nm, $c_{1,0} \simeq 10^{-2}$ g/g). [f] Extrapolated from other measurements by using $R_H \sim M_z^{0.55}$.

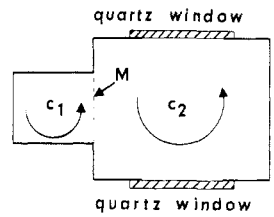

Figure 2. Schematic representation of the diffusion cell. The porous membrane M separates two compartments. The polymer molecules are initially introduced in compartment 1, and their diffusion through the membrane is followed by monitoring the concentration c_2 through the ultraviolet absorption of compartment 2. The concentrations c_1 and c_2 in both compartments are constantly homogenized by stirring.

3. Diffusion Cell. The diffusion cell is schematically represented in Figure 2. A porous membrane of 1-cm^2 area separates two compartments of respective volumes V_1 and V_2 (typically V_1 = 0.8 cm^3 and V_2 = 3.2 cm^3). Compartment 2 is equipped with two quartz windows that permit optical density measurements without dismounting the cell. Kalrez O-rings ensure tight seals and prevent solvent evaporation. Prior to the experiment, both compartments are carefully rinsed several times with filtered, freshly distilled solvent. Compartment 1 is then filled with a polymer solution at the initial concentration $c_{1,0}$, while compartment 2 is filled with pure solvent. Both compartments are completely filled to ensure constant volume conditions and tightly closed with Teflon seals to prevent solvent evaporation: as the solvent is incompressible, no osmotic bulk flow of solvent can take place. Under the osmotic pressure gradient established across the membrane, the polymer chains tend to diffuse and equilibrate the concentrations c_1 and c_2. In order to get well-defined limiting conditions for the diffusion, each compartment is constantly homogenized by small magnetic stirring bars. V_1 and V_2 are measured to a 1% accuracy by weighing. $c_{1,0}$ is determined by

ultraviolet absorption at 268 nm in a quartz cuvette of 1-mm optical path to an absolute accuracy of 5×10^{-3}OD. The relative uncertainty on $c_{1,0}$ is ±3% at 5×10^{-4}g/g and ±1.5% at $c_{1,0} = 10^{-3}$g/g. c_2 is monitored as a function of time through the ultraviolet absorption of compartment 2. Because of the long optical path of the cell (2 cm), there is an upper limit to the measurable concentration, $c_2 = 10^{-3}$ g/g, corresponding to an optical density of 3. For higher c_2 values, the experiment has to be stopped and the solution transferred from compartment 2 into a cell of shorter optical path.

Results

All the results presented here have been obtained with membranes of comparable geometrical characteristics: membrane thickness $L = 10$ μm, pore radius $R_P = 75$ nm, and total number of pores $N_P \sim 3 \times 10^8$. We have not been able to carry out reproducible and coherent measurements with smaller pore sizes ($R_P < 50$ nm). In particular, membranes with $R_P = 50$ nm strongly reject even very small molecular weight polymers ($M_W = 1.07 \times 10^5$, $R_H = 7.9$ nm). We have attributed this behavior to the important inhomogeneity of these small pores. In contrast, pore sizes much larger than 100 nm are not interesting if one wants to fulfill the condition $R_H > R_P$ without resorting to unpractically large polymer molecular weights. Keeping R_P fixed at 75 nm, we have varied the ratio $x = R_H/R_P$ between 0.105 and 1.47 with molecular weights in the range $M_W = 1.07 \times 10^5$–20.6×10^6.

To relate the observed evolution of the polymer concentration in compartment 2 with the diffusivity of the chains through the membrane it is of importance to check that the boundary condition of a uniform concentration in each compartment is achieved. An insufficient stirring may lead to the formation of boundary layers on each side of the membrane which increase the effective resistance to diffusion.

When the stagnant layer model as developed by Malone and Anderson[22] is used, the measured resistance of the membrane, R, ratio of the concentration difference between the two compartments to the flux of particles is the sum of the true membrane resistance R_m and the boundary layer resistance $2R_b$. $R_m = L/(p \times D_{eff})$, with D_{eff} the effective diffusion coefficient through the membrane and p the porosity. $R_b = \delta/D_0$ with D_0 the diffusion coefficient of the particles in free solution and δ the boundary layer thickness, $\delta \sim f^{-1/2}D_0^{1/3}$ (f is the stirring rate).

All the results presented here have been observed to be independent of the stirring rate within the experimental uncertainty (10%), for 50 rev/min < f < 200 rev/min. This means that in our experimental conditions R_b cannot exceed 20% of R_m. From the Malone and Anderson approach, $\rho = 2R_b/R_m = p(2\delta/L)(D_{eff}/D_0)$. In our experimental conditions we use membranes of low porosity $p <$ 5%. The boundary layer thickness can be estimated from the values of ρ measured by Bohrer:[23] for $f = 50$ rev/min and the smallest molecular weight we have used (comparable to the largest one used by Bohrer), we expect $\delta \simeq$ 20 μm. For the larger chains or for higher stirring rates, δ should decrease ($\delta \sim f^{-1/2}D_0^{1/3}$). Moreover, we expect an effective diffusion coefficient through the membrane D_{eff} much smaller than D_0, especially for R_p of the order of R_H. ρ should thus always stay smaller than 20%, in agreement with our observations.

Complementary experiments following the diffusion of smaller solutes in order to enhance the boundary layer effects are in progress in order to confirm the above analysis and lead to a more quantitative determination of the incidence of the stirring conditions.

1. Dilute Solutions. The evolution with time of the concentration in compartment 2, c_2, is presented in Figure 3 for several molecular weights. The solid lines represent the exponential laws

$$c_2 = c_{eq}(1 - e^{-t/\tau_{eff}}) \quad (1)$$

where c_{eq} is the equilibrium concentration ($c_{eq} = c_{1,0}V_1/(V_1 + V_2)$) and τ_{eff} is the effective diffusion time through the membrane. Such exponential kinetics, characteristic of a simple diffusion process, well describes the behavior of the two smaller molecular weights. The τ_{eff} values deduced from a best adjustment of eq 1 to our data are reported in Table II; they increase rapidly with the molecular weight. For the larger molecular weights, when R_H becomes comparable to R_P, the diffusion becomes strongly hindered: even for very long times ($t > 400$ h), the amount of polymer that has diffused through the membrane is very small, and the system does not reach the equilibrium concentration within attainable experimental times.

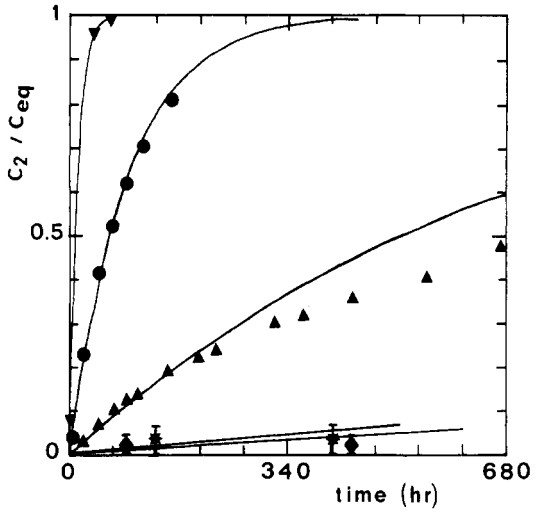

Figure 3. Normalized concentration in compartment 2, c_2/c_{eq}, as a function of time (c_{eq} is the equilibrium concentration) for polystyrene chains of different molecular weights diffusing through membranes of comparable porosity and of pore radius 75 nm: (▼) $M_W = 1.07 \times 10^5$; (●) $M_W = 7.75 \times 10^5$; (▲) $M_W = 2.89 \times 10^6$; (★) $M_W = 6.77 \times 10^6$; (♦) $M_W = 8.42 \times 10^6$. The solid lines are the predicted evolution for a simple diffusion process, $c_2/c_{eq} = 1 - \exp(-t/\tau_{eff})$, with the effective diffusion time through the membrane, τ_{eff}, adjusted to give the experimental initial variation. The corresponding τ_{eff} values, which strongly increase with molecular weight, are listed in Table II along with the corresponding initial concentrations $c_{1,0}$.

Table II
Effective Diffusion Time τ_{eff}[a]

M_W	$c_{1,0}$ g/g	R_H/R_P	τ_{eff}, h
1.07×10^5	10^{-3}	0.105	12 ± 1
7.75×10^5	9.1×10^{-4}	0.293	90 ± 5
2.89×10^6	9.9×10^{-4}	0.533	750 ± 200
6.77×10^6	1.1×10^{-3}	0.773	>7000
8.42×10^6	8.3×10^{-4}	0.993	>10000

[a] Through membranes of pore radius 75 nm and of comparable porosity for dilute solutions of different molecular weight M_W and initial concentrations $c_{1,0}$.

2. Concentration Effects. We have reported in Figure 4 the evolution of c_2 with time for different initial concentrations in compartment 1, $c_{1,0}$ (10^{-3}–2×10^{-2} g/g), and for $M_W = 6.77 \times 10^6$. Figures 5 and 6 present similar results for experiments performed in the same conditions but with $M_W = 8.42 \times 10^6$ and 20.6×10^6, respectively. In all cases, R_H is larger or comparable to R_P.

One can immediately see the drastic effect of the polymer concentration on the transport of the chains: for small $c_{1,0}$ only a negligible fraction of the polymer diffuses

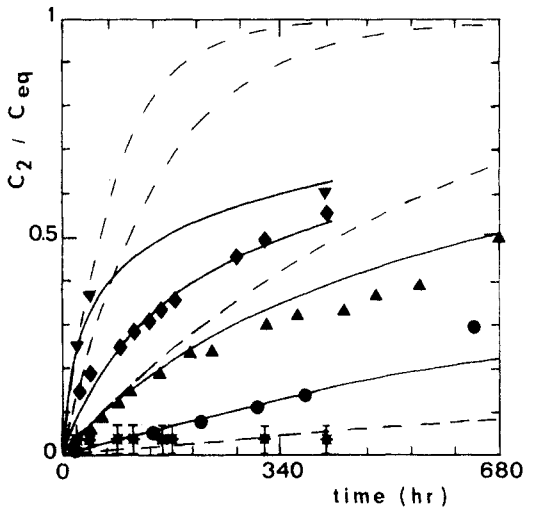

Figure 4. Normalized concentration c_2/c_{eq} as a function of time for $M_W = 6.77 \times 10^6$, $R_P = 75$ nm, and different initial concentrations $c_{1,0}$: (★) $c_{1,0} = 1.1 \times 10^{-3}$ g/g; (●) $c_{1,0} = 4.9 \times 10^{-3}$ g/g; (▲) $c_{1,0} = 7.1 \times 10^{-3}$ g/g; (♦) $c_{1,0} = 1.1 \times 10^{-2}$ g/g; (▼) $c_{1,0} = 1.93 \times 10^{-2}$ g/g. The dashed lines are the expected evolution for the simple diffusion process (effective diffusion coefficient through the membrane independent of concentration), $c_2/c_{eq} = 1 - \exp(-t/\tau_{eff})$, with τ_{eff} adjusted to give the experimental initial slopes. The solid lines are the calculated nonlinear solutions of eq 7 with the concentration-dependent effective diffusion coefficient of eq 6.

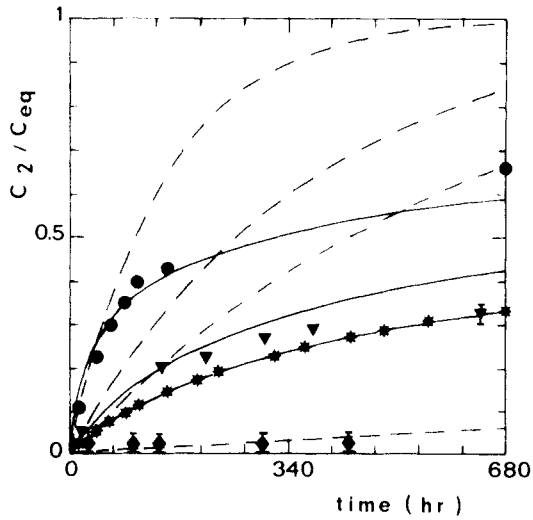

Figure 5. Same as Figure 4 except for $M_W = 8.42 \times 10^6$ and initial concentrations $c_{1,0}$: (♦) $c_{1,0} = 8 \times 10^{-4}$ g/g; (★) $c_{1,0} = 5 \times 10^{-3}$ g/g; (▼) $c_{1,0} = 10^{-2}$ g/g; (●) $c_{1,0} = 1.76 \times 10^{-2}$ g/g.

through the membrane, while for large enough $c_{1,0}$ more than 50% of the polymer can go through. This effect is not due to chain degradation by stirring or during the diffusion process, as evidenced by the QELS data taken before and after diffusion through the pores. Table I shows that R_H is only slightly affected by the diffusion. The 10% decrease in R_H observed for the $M_W = 8.42 \times 10^6$ sample could be due to a retention of the high molecular weight tail of the distribution.

An important point is that the kinetics of the diffusion when the transport is significant can no longer be described by the exponential law $c_2/c_{eq} = 1 - e^{-t/\tau_{eff}}$. This fact is evidenced by the dashed lines in Figures 4–6 where τ_{eff} has been adjusted to best agree with the experimental initial slopes. There is a marked slowing down of the diffusion as the experiment proceeds. The initial kinetics are nevertheless characterized by the τ_{eff} values, which are reported in Table III. We observe a decrease in τ_{eff} by more

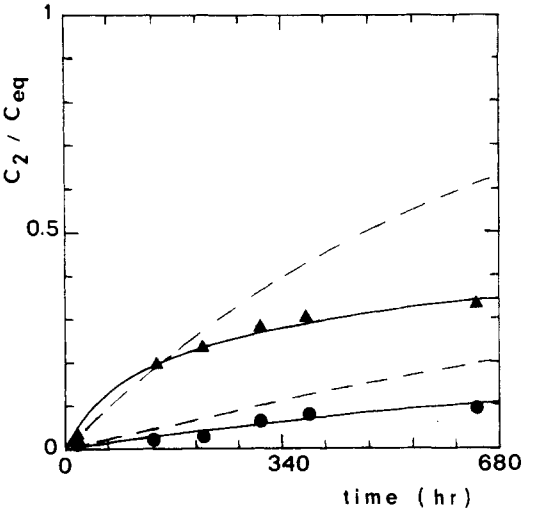

Figure 6. Same as Figure 4 except for $M_W = 20.6 \times 10^6$; $c_{1,0} = 5 \times 10^{-3}$ g/g (●) and 10^{-2} g/g (▲).

than 2 orders of magnitude for a 20-fold increase in $c_{1,0}$.

Discussion

1. Dilute Solutions. At low enough concentrations, the chains are isolated from each other and behave independently. As a consequence, the characteristic chain size to be compared to the pore size is the hydrodynamic radius R_H.

If the chains are considered as hard spheres, the effective diffusion coefficient through the membrane should follow the Renkin equation[24]

$$D_{eff}/D_0 = (1 - x)^2(1 - 2.1x + 2.1x^3 - 0.95x^5) \quad (2)$$

where $x = R_H/R_P$ and D_0 is the diffusion coefficient of one chain in free solution. The first factor of eq 2 is purely static and represents the probability for one chain to enter the pore, taking into account the steric hindrance at the pore wall. The second factor is dynamic in origin. It represents the slowing down of the diffusion due to the increased viscous drag experienced by the sphere inside the pore (the flow velocities must vanish at the pore wall).

From the data presented in Figure 3, we have deduced the effective diffusion time through the membrane, τ_{eff}. It is related to D_{eff} through geometrical factors characteristic of the membrane: $D_{eff} = A/\tau_{eff}$ with $A = L/[N_P\pi R_P^2(1/V_1 + 1/V_2)]$ (L is the membrane thickness and N_P its total number of pores). Throughout our experiments, all membranes are from the same batch, and A can be taken as constant. Since N_P is not precisely known, A has been determined experimentally by force fitting the results obtained with the smaller molecular weight sample ($M_W = 1.07 \times 10^5$) to eq 2: for $x = 0.105$, $D_{eff}/D_0 = 0.66$. This procedure leads to $A = 1.6 \times 10^{-2}$ cm^2, i.e., for $L = 10$ μm and $R_P = 75$ nm to $N_P = 2.4 \times 10^8$. This value is slightly smaller than expected from the irradiation dose.

The normalized effective diffusion coefficients D_{eff}/D_0 thus deduced are compared to eq 2 in Figure 7. The agreement seems quite good except for x close to 1 where we observe an effective diffusion coefficient more than two times larger than predicted for hard spheres. Although this may be due to a trivial polydispersity effect, it may also have a profound physical significance. When R_H is comparable to R_P, the hard-sphere model becomes inadequate and the chain flexibility should play an important role.

The conformations of flexible chains trapped in cylindrical pores and in good solvent conditions have been

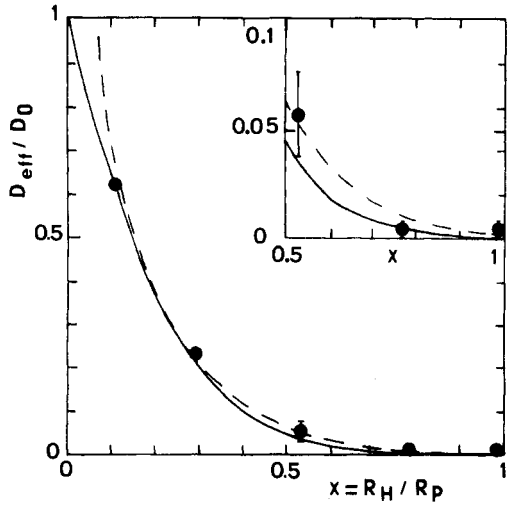

Figure 7. Normalized effective diffusion coefficient through the membrane D_{eff}/D_0 (D_0 is the diffusion coefficient in the bulk solution) as a function of the ratio of the hydrodynamic radius of the chains to the pore radius, $x = R_H/R_P$, for several molecular weights, $R_P = 75$ nm, and initial concentrations $c_{1,0}$ in the dilute range. The full line is the Renkin equation (eq 2) and the dashed line the scaling prediction of eq 4 with $\alpha = 2.5$ and $B = 0.32$. As evidenced by the insert, the scaling prediction leads to $D_{eff}/D_0 \neq 0$ for $x \simeq 1$.

worked out by Daoud and de Gennes.[14] For dilute chains in the pores, they have shown that the chains stay as spherical coils for x smaller than 1 but become elongated cigars at large x. When the chains have the shape of elongated cigars, the excluded-volume interactions are screened out over distances comparable to R_P. The partition coefficient K, ratio of the concentration inside the pore c_P to the concentration in the bulk solution c_B, can be evaluated from the loss of entropy of the chains when they become confined into the pore. K is expected to depend only on x: $K(x) = c_P/c_B = \exp(-x^{5/3})$.[14] The dynamic properties of such chains have been studied by Brochard and de Gennes.[16] They have shown that the hydrodynamic interactions should also be screened out over R_P, which leads to a decrease of the diffusion coefficient inside the pore, $D_{pore} = D_0 f(x)$ with $f(x) = x^{-2/3}$ for $x > 1$ and $f(x) = 1$ for x going to 0. When the two predictions are coupled, the effective diffusion coefficient through the membrane should follow, for large enough x, the scaling law

$$D_{eff}/D_0 = Bx^{-2/3} \exp(-x^{5/3}) \quad (3)$$

where B is a proportionality constant. Contrary to eq 2, eq 3 predicts a small but nonzero value of the effective diffusion coefficienct for R_H/R_P close to 1, as observed experimentally. A precise and quantitative test of eq 3 is, however, difficult to perform: eq 3 is deduced from scaling arguments, and, as usual, prefactors are omitted. One should look rather for a parametrized form

$$D_{eff}/D_0 = Bf(\alpha x)K(\alpha x) \quad (4)$$

where α is a second proportionality constant. In their earlier work, Cannell and Rondelez[10] had obtained $\alpha = 2.5$ from a best fit of eq 4 to their experimental points in the range $x < 0.8$. The dashed line in Figure 7 represents eq 4 with the same value $\alpha = 2.5$ and B adjusted to 0.32 to best fit our data. It is clear that eq 4 can describe the data. However, the improvement with respect to Renkin's curve is not obvious, and at this stage we cannot separate clearly between the two approaches.

One can notice in Figure 3 that for $M_W > 2.89 \times 10^6$ the kinetics of the diffusion significantly deviates from a single exponential. A detailed analysis is presently under way to determine whether this nonexponential behavior has to be attributed to polydispersity or to a variation of the hydrodynamic radius of the chains as $c_1(t)$ decreases during the experiment (second virial coefficient effect).

2. Semidilute Solutions. Our most striking experimental result is the strong increase in the efficiency of the diffusion when the initial concentration is increased. It is now well-known that for concentrations larger than the crossover concentration for chain overlap, c_B^*, the diffusion under an osmotic pressure gradient, in a free solution, is governed by the cooperative diffusion coefficient, D_{coop}, which is an increasing function of concentration.[25] However, this factor alone cannot explain the observed D_{eff} variation by 2 orders of magnitude in the concentration range 10^{-3}–2×10^{-2} g/g. According to the quasi-elastic light scattering measurements of ref 26 and the scaling law $D_{coop} = D_0(c_B/c_B^*)^{3/4}$, one only expects a factor of 5 change in D_{coop} for our experimental semidilute ranges. This suggests that partitioning between free solution and pores should play an important role.

The partition coefficient has been evaluated by Daoudi and Brochard[15] for concentrations where the chains are entangled both in the free solution and inside the pore. In this regime, the relevant parameter characterizing the conformation of the chains is no longer their hydrodynamic radius but the average distance between entanglements ξ, which represents the screening length for both excluded volume and hydrodynamic interactions; ξ only depends on concentration as $\xi \sim c_B^{-3/4}$. For $\xi < R_P$, K should be much larger than in the dilute case and asymptotically reach the value of 1 when ξ becomes comparable to a monomer size. Since the concentration inside the pore, c_P, is always smaller than c_B, one should also expect a regime in which the chains are entangled outside the pore but are still dilute elongated cigars inside the pores. This intermediate regime has not yet been considered and corresponds to $R_H > \xi > R_P$ in the bulk solution. Following ref 15, we can write the chemical potential of one chain outside the pore (conventional semidilute solution)

$$\mu_{SD} = kT[\ln c_B + N/c_B\xi^3] = kT[\ln c_B + (c_B/c_B^*)^{5/4}]$$

and inside the pore (dilute cigars) as

$$\mu_P = kT(\ln c_P + x^{5/3})$$

At equilibrium these chemical potentials have to be equal, and the partition coefficient will depend on concentration as

$$K(c_B) = \exp[-x^{5/3} + (c_B/c_B^*)^{5/4}] = K_{dilute} \exp(c_B/c_B^*)^{5/4} \quad (5)$$

We notice that eq 5 crosses over smoothly toward K_{dilute} for $c_B = c_B^*$ and toward $K_{semidilute}$[14,15] for $c_B = c_1$ where c_1 is defined by $\xi(c_1) = R_P$ or $c_1 = c_B^*(R_H/R_P)^{4/3}$. With the scaling predictions for c_B^* and R_H,[27] $c_1 \sim (a/R_P)^{4/3}(1/a^3)$, where a is a monomer size. c_1 is independent of the chain size. As in this intermediate regime the chains are dilute inside the pore, their diffusion coefficient in the pore still obeys $D_{pore} = D_0 x^{-2/3}$ as noted under Dilute Solutions. The effective diffusion coefficient through the membrane should then be

$$D_{eff}(c_B) = K(c_B)D_{pore}$$

$$D_{eff}(c_B) = D_{eff,dilute} \exp[+(c_B/c_B^*)^{5/4}] \quad (6)$$

$D_{eff,dilute} = K_{dilute}D_{pore}$ is the effective diffusion coefficient at infinite dilution for a given molecular weight and given membrane.

Table III
Characteristics of Diffusion for Semidilute Solutions of Large Molecular Weights at Different Initial Concentrations $c_{1,0}$ through Membranes of Pore Radius 75 nm and of Comparable Porosity[a]

$c_{1,0}$ g/g	τ_{eff}, h	$\tau(c_{1,0})$, h	c_B^*, g/g
	$M_W = 6.77 \times 10^6$		
1.1×10^{-3}	>7000		
4.9×10^{-3}	2000 ± 500	2300 ± 370	$(4.5 \pm 0.5) \times 10^{-3}$
7.1×10^{-3}	490 ± 180	570 ± 70	$(4.5 \pm 0.5) \times 10^{-3}$
1.1×10^{-2}	154 ± 8	170 ± 20	$(4.5 \pm 0.5) \times 10^{-3}$
1.93×10^{-2}	95 ± 5	35 ± 4.5	$(4.5 \pm 0.5) \times 10^{-3}$
	$M_W = 8.42 \times 10^6$		
8.3×10^{-4}	>8000		
5.1×10^{-3}	500 ± 40	685 ± 80	$(1.5 \pm 0.25) \times 10^{-3}$
10^{-2}	355 ± 20	450 ± 70	$(3.5 \pm 0.5) \times 10^{-3}$
1.76×10^{-2}	150 ± 10	70 ± 20	$(4.5 \pm 0.5) \times 10^{-3}$
	$M_W = 20.6 \times 10^6$		
5.5×10^{-3}	2340 ± 550	3600 ± 800	$(1.9 \pm 0.2) \times 10^{-3}$
10^{-2}	540 ± 150	270 ± 50	$(1.9 \pm 0.2) \times 10^{-3}$

[a] τ_{eff} corresponds to an exponential diffusion law adjusted to the initial slope (dashed lines in Figures 4–6), and $\tau(c_{1,0})$ is the initial diffusion time deduced from the best fit of eq 6 on our data (solid lines in Figures 4–6). $\tau(c_{1,0})$ depends on the initial concentration as $\exp[-(c_{1,0}/c_B^*)^{5/4}]$. The last column gives corresponding c_B^* values deduced from the fit.

Equation 6 implies that $c_1(t)$ and $c_2(t)$ obey highly nonlinear diffusion laws, which we may write in first approximation, neglecting the concentration variation inside the pore:

$$\frac{dc_1}{dt} = -D_{eff}(c_1)\frac{c_1 - c_2}{A}\frac{V_2}{(V_1 + V_2)}$$

$$\frac{dc_2}{dt} = -\frac{V_1}{V_2}\frac{dc_1}{dt} \qquad (7)$$

$$c_2(t) = [c_{1,0} - c_1(t)]\frac{V_1}{V_2}$$

We have calculated c_1 and c_2 point by point by numerical integration of eq 7, using time intervals of 1 h and a simple algorithm derived from the Euler method. The calculated curves have been adjusted onto the experimental data points of Figures 4–6, taking as parameters $D_{eff}(c_{1,0})$ and c_B^*, and are shown as solid lines. One can immediately see that the nonexponential shape of $c_2(t)$ is well accounted for when the effective diffusion coefficient described by eq 6 is used. However, the fitting procedure is not sensitive to the exact value of the exponent of the power law inside the exponential. Changing this exponent leads to equally good fits, with new sets of adjustable parameters $D_{eff}(c_{1,0})$ and c_B^*. A test of the model is, then, to compare the best-fitted values for $\tau(c_{1,0}) = A/D_{eff}(c_{1,0})$ and c_B^* with their physical interpretation. The values of these two parameters, obtained with the effective diffusion coefficient given by eq 6, are reported in Table III.

c_B^* has to be identified with the crossover concentration between dilute and semidilute regimes and should depend on the molecular weight of the chains as $c_B^* \sim M_W^{-4/5}$ (good solvent conditions).[25] Table III shows that except for one experiment ($M_W = 8.42 \times 10^6$, $c_{1,0} = 5.1 \times 10^{-3}$ g/g) we do obtain c_B^* values which only depend on the molecular weight and are compatible with the above scaling law. It can also be checked that the absolute values are comparable to those deduced from elastic light scattering data[28] (see Table I). A possible explanation for the discrepancy observed at $M_W = 8.42 \times 10^6$, $c_{1,0} = 5.1 \times 10^{-3}$ g/g is an anomalously high porosity for that particular membrane. This fact is confirmed by the value of $\tau(c_{1,0})$, which is too small by a factor of 4 with respect to the other results. Although a high porosity should in principle not affect c_B^*, interconnected pores could lead to an "activation" of the diffusion.

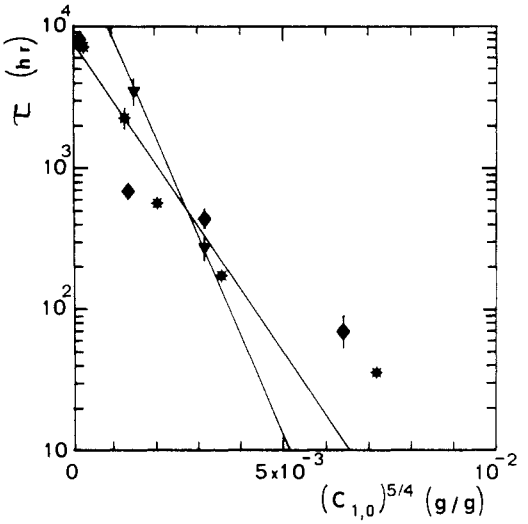

Figure 8. Plot of the adjusted initial diffusion time through the membrane, $\tau(c_{1,0})$, in log scale, as a function of $(c_{1,0})^{5/4}$ for the three different studied molecular weights, $M_W = 6.77 \times 10^6$ (★), 8.42×10^6 (♦), and 20.6×10^6 (▼). Taking into account the large uncertainty in $\tau(c_{1,0})$, a qualitative agreement with eq 8 is observed, except for the largest initial concentrations for which a crossover toward a regime where the polymer chains are entangled inside the pores may start to be visible.

Similarly, following eq 6, we expect $\tau(c_{1,0})$ to depend on molecular weight and initial concentration $c_{1,0}$ as

$$\tau(c_{1,0}) = \frac{A}{D_{eff,dilute}} \exp[-(c_{1,0}/c_B^*)^{5/4}] \qquad (8)$$

In Figure 8 we have reported $\tau(c_{1,0})$ in log scale as a function of $(c_{1,0})^{5/4}$. Equation 8 is qualitatively obeyed for $c_{1,0} < 1 \times 10^{-2}$ g/g. The slopes yield c_B^* values of $(4.5 \pm 0.5)10^{-3}$ g/g and $(2.6 \pm 0.2)10^{-3}$ g/g for $M = 6.77$ and 20.6×10^6, respectively, which are comparable to the values shown in Table III. In contrast, for a given initial concentration, $\tau(c_{1,0})$ increases with molecular weight more slowly than predicted by eq 8 and 3 (1 order of magnitude instead of 2 for M_W going from 6.77×10^6 to 20.6×10^6, in the range 5×10^{-3} g/g $< c_{1,0} < 10^{-2}$ g/g). Two experimental limitations may explain this discrepancy: first, it is very difficult to measure with accuracy characteristic diffusion times longer than 1000 h; second, the polydispersity of the polymer may influence the results, especially for the highest molecular weight samples.

For $c_{1,0} \simeq 2 \times 10^{-2}$ g/g, the $\tau(c_{1,0})$ values deviate from eq 8. This trend most likely reflects the proximity of the high-concentration regime where the chains become semidilute inside the pore and are no longer strongly excluded from the pores ($K(c_{1,0})$ close to 1). Indeed, for this high $c_{1,0}$, the $\tau(c_{1,0})$ values are comparable to the diffusion time τ_0 obtained for unrestricted diffusion. Typically, close to c_B^*, $\tau_0 = A/D_{coop} \simeq A/D_0$. With the D_0 values deduced from Table I, we obtain $\tau_0 = 58$ h and 75 h for $M_W = 6.77 \times 10^6$ and 8.42×10^6, respectively, while the corresponding $\tau(c_{1,0})$ values are 35 h and 70 h.

Conclusion

We have undertaken systematic studies of the diffusion of large flexible polymer molecules through model porous membranes for a large range of molecular weights (1.07×10^5 to 20.6×10^6) and polymer concentrations (5×10^{-4} g/g to 2×10^{-2} g/g). The regime of interest where the

hydrodynamic radius of the chain R_H is comparable or larger than the pore radius R_P has been particularly investigated. Due to experimental limitations involved in the fabrication of well-controlled membranes with small pores ($R_P < 50$ nm), all results presented here have been obtained with membranes of pore radius 75 nm. Depending upon the initial polymer concentration, we have observed two very different diffusion behaviors:

In the dilute regime, the diffusion of the chains is highly hindered when R_H becomes comparable to R_P. The effective diffusion coefficient of the chains through the membrane D_{eff} is a function of $x = R_H/R_P$. The results are equally well described by the hard-sphere model or the scaling law approach for flexible chains.

At large enough concentrations, diffusion of otherwise blocked chains becomes permitted. The diffusion kinetics are highly nonexponential and concentration dependent. To explain this behavior, we propose a model in which the chains are entangled outside the pores and dilute (elongated cigars) inside the pore. The diffusion process is then completely dominated by the concentration dependence of the partition coefficient $K = c_P/c_B$, where c_P and c_B are the polymer concentrations inside the pore and in the bulk solution, respectively. Scaling arguments lead to $K = K_{dilute} \exp[(c_B/c_B^*)^{5/4}]$, where c_B^* is the crossover concentration between dilute and semidilute regimes. This model well describes the nonexponential kinetics of diffusion. It is also in good qualitative agreement with both the molecular weight and the concentration dependence of the measured initial effective diffusion coefficient through the membrane.

At the highest concentration studied ($c_{1,0} = 2 \times 10^{-2}$ g/g), a regime in which the diffusion is almost unhindered by the pores seems to appear.

Further experiments are presently under way to test the scaling law predictions in more detail, especially for the transition between the intermediate and the high concentration regimes, which should not depend upon molecular weight but only on pore size and concentration.

Acknowledgment. We are very much indebted to F. Brochard, P. G. de Gennes, and J. F. Joanny for illuminating discussions and to G. Chauveteau and M. Bagassi for constant communication, prior to publication, of their own results on transport under flow.

Registry No. Makrofol, 24936-68-3; polystyrene (homopolymer), 9003-53-6.

References and Notes

(1) Satterfield, C. N.; Colton, C. K.; Pitcher, W. H. *AIChE J.* **1973**, *19*, 628.
(2) Colton, C. K.; Satterfield, C. N.; Lai, C. J. *AIChE J.* **1975**, *21*, 289.
(3) Haller, W. *Macromolecules* **1977**, *10*, 83.
(4) Beck, R. E.; Schultz, S. J. *Biochim. Biophys. Acta* **1972**, *255*, 273.
(5) Schultz, J. S.; Valentine, R.; Choi, C. Y. *J. Gen. Physiol.* **1979**, *73*, 49.
(6) Long, T. D.; Jacobs, D. L.; Anderson, J. L. *J. Membr. Sci.* **1981**, *9*, 13.
(7) Zeman, L.; Wales, M. *Sep. Sci. Technol.* **1981**, *16*, 275.
(8) Chauveteau, G. *J. Rheol.* **1982**, *26*, 111. Chauveteau, G.; Tirrell, M.; Omari, A. *J. Colloid Interface Sci.* **1984**, *100*, 41.
(9) Satterfield, C. N.; Colton, C. K.; de Turckheim, B.; Copeland, T. M. *AIChE J.* **1978**, *24*, 937.
(10) Cannell, D.; Rondelez, F. *Macromolecules* **1980**, *13*, 1599.
(11) Long, T. D.; Anderson, J. L. *J. Polym. Sci., Polym. Phys. Ed.* **1984**, *22*, 1261.
(12) Bagassi, M.; Chauveteau, G., private communication.
(13) (a) Casassa, E. F. *J. Polym. Sci., Part B* **1967**, *5*, 773. (b) Casassa, E. F. *J. Polym. Sci., Polym. Phys. Ed.* **1972**, *10*, 381. (c) Casassa, E. F. *Macromolecules* **1976**, *9*, 182.
(14) Daoud, M.; de Gennes, P. G. *J. Phys. (Les Ulis, Fr.)* **1977**, *38*, 85.
(15) Daoudi, S.; Brochard, F. *Macromolecules* **1978**, *11*, 751.
(16) Brochard, F.; de Gennes, P. G. *J. Chem. Phys.* **1977**, *67*, 52.
(17) Long, T. D.; Anderson, J. L., private communication.
(18) Guillot, G.; Rondelez, F. *J. Appl. Phys.* **1981**, *52*, 7155.
(19) Crawford, W. T.; de Sorbo, W.; Humphrey, J. S. *Nature (London)* **1968**, *220*, 1313.
(20) de Sorbo, W. *Nucl. Tracks* **1979**, *3*, 13.
(21) Adam, M.; Delsanti, M. *Macromolecules* **1977**, *10*, 1229.
(22) Malone, D. M.; Anderson, J. L. *AIChE J.* **1977**, *23*, 177.
(23) Bohrer, M. P. *Ind. Eng. Chem. Fundam.* **1983**, *22*, 72.
(24) Renkin, E. M. *J. Gen. Physiol.* **1954**, *38*, 225. See also the review by Bean, C. P. in "Membranes, A Series of Advances"; Eisenman, G., Ed.; Wiley: New York, 1972; Vol 1.
(25) Adam, M.; Delsanti, M.; Pouyet, G. *J. Phys., Lett.* **1979**, *40*, L-435.
(26) Brown, W. "Proceedings of the 27th Microsymposium on Macromolecules, IUPAC, Prague, July 1984"; Sedlacek, Ed.; Pergamon: Oxford, 1984.
(27) de Gennes, P. G. In "Scaling Concepts in Polymer Physics"; Cornell University Press: Ithaca, NY, 1979; Chapter III, p 76.
(28) Munch, J. P.; Candau, S.; Herz, J.; Hild, G. *J. Phys. (Les Ulis, Fr.)* **1977**, *38*, 971.